Imaging the TiO_2(011)-(2×1) Surface using Noncontact Atomic Force Microscopy and Scanning Tunneling Microscopy

Ayhan Yurtsever[†,‡,*], Jo Onoda[§,||], Masayuki Abe[‡], Chi Lun Pang[⊥,*], Yoshiaki Sugimoto[§,||]

[†]Institute of Scientific and Industrial Research, Osaka University, 8-1 Mihogaoka, Ibaraki, Osaka 567-0047, Japan, [‡]Graduate School of Engineering Science, Osaka University, 1-1 Machikaneyama, Toyonaka, Osaka 560-0043, Japan, [§]Graduate School of Engineering, Osaka University, 2-1 Yamada-Oka, Suita, Osaka 565-0871, Japan, [||] Department of Advanced Materials Science, University of Tokyo, 5-1-5 Kashiwanoha, Kashiwa, Chiba 277-8561, Japan, [⊥] Department of Chemistry and London Centre for Nanotechnology, University College London, London WC1H 0AJ, United Kingdom.

*Corresponding authors:

Dr. Ayhan Yurtsever

Tel: +81-6-6850-6304

Fax: +81-6-6850-6662

E-mail: ayhan@afm.eei.eng.osaka-u.ac.jp.

Dr. Chi Lun Pang

Tel: +44-207-679-5580.

Fax: +44-207-679-0595.

E-mail: chi.pang@ucl.ac.uk.

ABSTRACT

We have used noncontact atomic force microscopy (NC-AFM) and scanning tunneling microscopy (STM) to study the rutile TiO_2(011)-(2×1) surface. NC-AFM images were obtained with several different contrasts. In particular, a zigzag contrast similar to that found in STM was observed. Simultaneously-recorded NC-AFM and STM images indicate that the zigzags in NC-AFM and STM are in phase and may therefore have a similar origin. Hydrogen adatoms were also identified in NC-AFM images by comparison with STM. Sequential NC-AFM scans of the same area show that these hydrogen atoms readily diffuse between adjacent topmost oxygen atoms and follow a zigzag path, thus indicating that the H adatoms adsorb on either side of the (2×1) rows.

INTRODUCTION

TiO_2 has been investigated intensely for several decades since the discovery that it is an active photocatalyst.[1] This has led to numerous surface science studies focused mainly on the most thermodynamically stable rutile TiO_2(110) face.[2,3] However, recently, there has also been considerable interest in other rutile faces [4-18] as well as anatase and layered TiO_2 phases.[19-23] Rutile TiO_2(011) has received considerable attention due to reports of an enhanced photoactivity compared with other rutile phases.[24,25]

In the most part, studies of TiO_2(011) focus on the (2×1) reconstruction which forms after typical ultrahigh vacuum (UHV) sample preparation.[3,5-12,14-16] After two models were proposed based on scanning probe microscopy studies,[5,6] three diffraction studies support the same 'diffraction model' shown in Figure 1a,b.[9-11] Theoretical calculations also find this to be the most stable of the proposed models.[9,10] In scanning tunneling microscopy (STM) images, '*beanlike*' and '*zigzag*' motifs appear in images recorded 'close to' and 'far from' the surface respectively,[10,15] and both these could be reproduced by STM images simulated from the 'diffraction model'.[15]

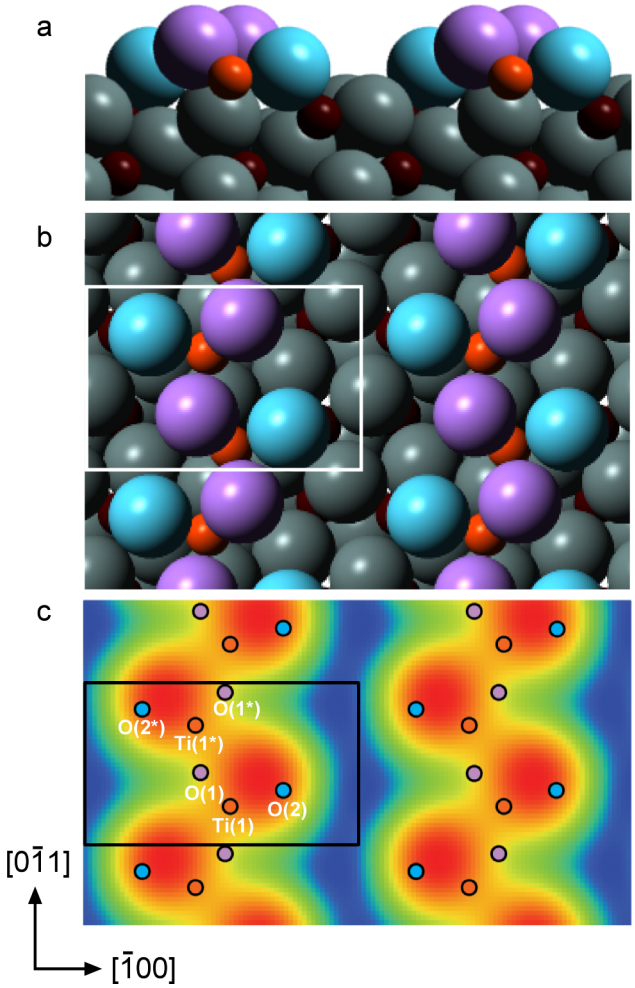

Figure 1 (a) Side view of the ball model of TiO_2(011)-(2×1) viewed along the [0$\bar{1}$1] direction. **(b)** Top view of the same model. The top layer O atoms are shown purple and the second layer light blue. All other O atoms are shown grey. The top Ti atoms are shown orange whereas all other Ti are shown dark red. **(c)** Simulated STM image of the TiO_2(011)-(2×1) surface with the top atoms of the model superimposed, adapted with permission from ref. (15).

Our understanding of the structure and reactivity of TiO_2(110) has been advanced by the application of NC-AFM as well as the related technique of Kelvin probe force microscopy (KPFM). For example, NC-AFM imaging and force

spectroscopy measurements together with density functional theory calculations revealed that the AFM contrast for Pt and other metallic adsorbates reflects their chemical reactivity and provides an explanation for the important role they play in catalysis,[26] simultaneous NC-AFM/STM has revealed the presence of subsurface hydrogen,[27] and KPFM studies indicate an electron charge transfer to the TiO_2(110) surface in the case of adsorbed Na and K atoms[28,29] and electron transfer from the surface in the case of Au nanoparticles.[30]

On the other hand, there are only two NC-AFM studies of the TiO_2(011) surface.[6,31] Previously in NC-AFM, the (2×1) phase was imaged as broad, bright rows without sufficient resolution to reveal any sub-row structure.[6] In that same study,[6] a co-existing (4×1) phase was also reported. Based on recent high resolution NC-AFM and STM images, we proposed models for a series of (2*n*×1) models, including two (4×1) phases, that have the same structural elements as the (2×1) phase.[31] In the present article, we use NC-AFM to image the TiO_2(011)-(2×1) reconstruction for the first time with atomic resolution. As on TiO_2(110), NC-AFM imaging of this surface gives rise to several types of contrast, one of which appears almost identical to the zigzag contrast common in STM images of TiO_2(011)-(2×1). Simultaneously-recorded NC-AFM/STM images reveal that the NC-AFM and STM zigzags are in-phase with each other and therefore may have a similar origin. Likewise, by comparison with STM images, hydrogen adatoms are clearly identified in the NC-AFM images. Sequential NC-AFM images taken from the same area give the first direct experimental evidence that these H atoms readily diffuse between adjacent topmost oxygen atoms and follow a zigzag path, thus indicating that the H adatoms adsorb on either side of the (2×1) rows.

EXPERIMENTAL METHODS

The experiments were performed in Osaka and Tokyo using a custom-built NC-AFM housed in an UHV chamber (with a base pressure of ~5×10^{-11} Torr) and operated at room temperature. The TiO_2(011) crystal (*MaTecK GmbH*) was prepared using repeated cycles of Ar-ion bombardment (2 keV) for approximately 5 min and annealing between 943-953 K for 10-25 min which gave the (2×1) terminations.

NC-AFM images were obtained using the frequency modulation detection method,[32] with the cantilever oscillation amplitude kept constant (peak-to-peak amplitudes 220-270 Å). The data presented here were taken using silicon cantilevers which had resonant frequencies in the range ~293-331 kHz. A DC voltage (V_{CPD}) is added between the tip and sample that minimizes the average tip-sample contact potential difference.

In Fig. 2, the STM images were obtained using the same cantilevers, biased with a voltage (V_s) and with the oscillation switched off. In some cases, the tips were treated by electrical pulses or nanoindentation procedures to ensure sufficient conductivity for STM measurements.

Simultaneous NC-AFM and STM images were obtained by measuring the retrace image in the constant height mode and detecting Δf together with the time-averaged current, $\bar{I}_t$. This eliminates any crosstalk between the topography and the time-averaged current, $\bar{I}_t$, which would otherwise act to give a current map that is out-of-phase compared with the topography.[33]

RESULTS AND DISCUSSION

Figure 2 shows a topographic NC-AFM image of the TiO_2(011)-(2×1) surface together with the Δf and $\bar{I}_t$ maps which were recorded simultaneously in the retrace scan. All three images have a zigzag contrast similar to that reported in several STM studies of the TiO_2(011)-(2×1) surface (refs. 3,5-8,10,12-16) as well as NC-AFM images of the TiO_2(011)-(2n×1) phases.[31] Two guidelines as well as a zigzag and a triangle are drawn on the Δf map in Figure 2b and these are superimposed onto the $\bar{I}_t$ map. In both images, the black guidelines run along the bright zigzag rows whereas the white guidelines run between the bright zigzag rows. Likewise, the turning points of the zigzags and the apices of the triangles lie on bright spots in both the Δf and $\bar{I}_t$ maps. This indicates that the two images are in phase with each other.

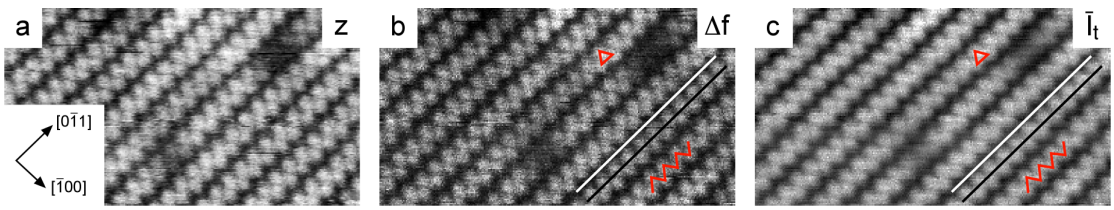

Figure 2 Simultaneously-acquired 100 Å × 55 Å NC-AFM images of TiO_2(011)-(2×1). **(a)** Topographic NC-AFM image recorded with constant Δf = -15.8 Hz, V_s = 1.8 V. **(b)** Δf map recorded in a retrace scan in the constant height mode. **(c)** $\bar{I}_t$ map recorded in a retrace scan in the constant height mode. Black and white guidelines as well as red triangles and zigzags are drawn to highlight the registry between the images in (b) and (c).

Figure 1c shows the STM simulation for the zigzag mode from ref (15) on which a plot of the topmost atoms, O(1,1*), Ti(1,1*), and O(2,2*) is superimposed.

The simulated STM image shows that the bright spots are centered between the oxygen in the second layer, O(2) and O(2*), and the topmost titanium, Ti(1) and Ti(1*). Given that the zigzags in the NC-AFM image are in phase with those in the STM image, this means that the bright spots in NC-AFM must also be positioned between the second layer of oxygen and the topmost layer of Ti. In STM, the zigzag contrast is dominated by tunneling into Ti 3*d* states because of its longer decay length compared to the O 2*p* states.[15] Furthermore, the roundness of the bright spots in the zigzag mode could only be reproduced when tip convolution was allowed by explicitly including a finite-sized tip in the simulation.[15] The zigzag STM contrast is largely electronic, so one would not necessarily expect that a similar contrast would be seen in NC-AFM. That an almost identical zigzag contrast is found in the NC-AFM images may be due to an interplay between the decay of the tip−sample potential and the surface geometry as well as tip convolution and atomic relaxation effects.[34] Theoretical simulation of the NC-AFM images would shed more light on this.

In the majority of our NC-AFM and STM images of the surface, defects can be observed with coverages of ~0.04-0.08 monolayer (ML), where 1 ML is the concentration of TiO_2(011) (1×1) surface unit cells. Depending on the tip condition, the defects can appear bright or dark. Figure 3a shows an STM image that contains a number (~0.05 ML) of small bright spots that make up the vast majority of the defects, together with a small number of unknown, larger, brighter defects. According to Tao *et al*. the major point defects on this surface are hydrogen adatoms,[14] with calculations showing that the hydrogen adsorbs on the topmost oxygen, i.e. at O(1) or O(1*). In their highest resolution STM images, Tao *et al*.[14] observe an offset of ~1 Å along the [$\bar{1}$00] direction between hydrogen adsorbed either side of the zigzag, i.e. at

O(1) or O(1*). This offset is rather close to the separation of ~0.9 Å between these topmost O atoms. Figure 3b shows a high resolution STM image of the TiO_2(011)-(2×1) surface where an offset of ~1.3 Å along [$\bar{1}$00] can be observed between bright defects. As such, we conclude that the small, bright defects in Figure 3 are also hydrogen adatoms, in line with the assignment of Tao *et al.*[14]

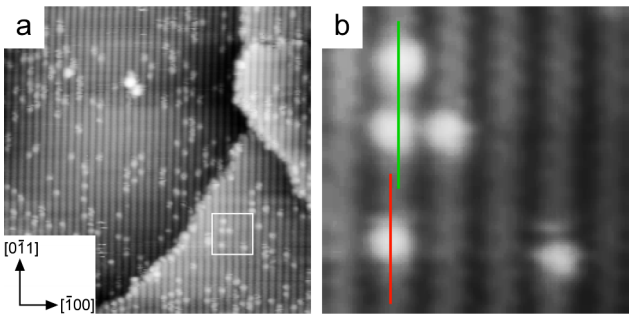

Figure 3 (a) (375 Å)^2 STM image of TiO_2(011)-(2×1) with V_s = 2 V and I_t = 0.03 nA. **(b)** (47.5 Å)^2 STM image magnified from the square indicated in (a). In (b), red and green guidelines are drawn to highlight the offset between the bright defects in the [$\bar{1}$00] direction.

Figure 4 shows three NC-AFM images recorded sequentially from the same area together with duplicate images where the H adatoms are marked. The contrast between these images is different and we attribute this to changes in the precise atomic configuration of the tip apex, different tip-sample separations, or a combination of both. In Figure 4a,b the rows are resolved into zigzag spots although the contrast is weak. In Figure 4c,d the rows are very clearly resolved into a zigzag arrangement of spots. In Figure 4e,f the (2×1) rows are imaged as broad featureless rows, without any sub-row resolution.

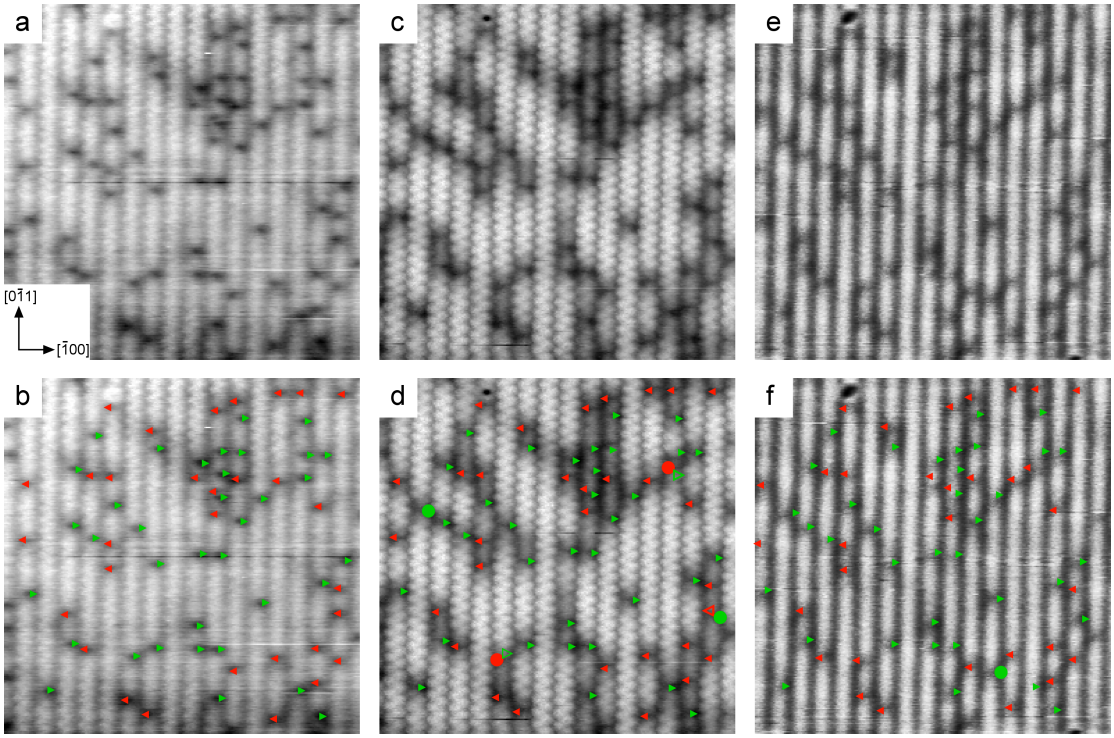

Figure 4 Sequential (150 Å) NC-AFM images (V_{CPD} = 1 V) of the TiO_2(011)-(2×1) surface showing different contrasts and decorated with 0.08 ML H adatoms with Δf = **(a)** -5.5 Hz, **(c)** -7.0 Hz, and **(e)** -6.2 Hz. **(b,d,f)** As (a,c,e) with defects highlighted. Green, filled triangles pointing to the right indicate defects offset to the right; red, filled triangles pointing to the left indicate defects offset to the left. In (d), defects that are missing compared to the image in (b) are marked with open triangles. Defects that are present in (d) but not (b) and those that are present in (f) but not (d) are highlighted with filled circles.

The appearance of H adatoms also varies amongst these images. In Figure 4a, the hydrogen adatoms appear as dark spots offset to one side of the row. In the duplicated image in Figure 4b, the hydrogen atoms offset to the right-hand side are highlighted with green triangles that point to the right whereas those offset to the left-hand side are highlighted with red triangles that point to the left. In total there are 37

hydrogen atoms offset to the right and 31 to the left, close to what one would expect from a random distribution.

In Figure 4d, the green and red triangles highlight the same features with a few exceptions. The open red and green triangles indicate where a hydrogen atom present in Figure 4a is absent in Figure 4c. In both cases, an extra H adatom is found diagonally adjacent to where the missing H adatom was located, indicative of H adatom diffusion. These H adatoms are highlighted with red and green circles. One further H adatom also appears in Figure 4c and is highlighted with a green circle. We assume that this new H adatom also appears due to diffusion, presumably from outside the frame or from the tip given that we cannot identify the original position in Figure 4a.

The H adatoms have a peculiar contrast in Figure 4c,d. When several H adatoms are nearby, a number of the sites surrounding the dark spots from the H adatoms are also significantly darker than the bare rows. It may be that the tip in Figure 4c is particularly charged and is therefore repelled from several H adatoms that are in close vicinity. The markers from Figure 4d are plotted onto the NC-AFM image in Figure 4f. While these markers fall on dark spots, the H adatoms tend towards a dumbbell-like shape with dark spots either side of the bright spot.

As on the TiO_2(110) surface,[33-37] we have observed several other NC-AFM contrasts which are summarized in Fig. S1, including a 'hidden' mode where the H adatoms are not visible (Fig. S1a), a 'protrusion' mode (Fig. S1b) where the H adatoms appear bright, and two atomically-resolved modes (Figs. S1c,d) where the H adatoms are dark. In the hidden mode, we believe that the H adatoms are present but not imaged as has been observed previously for TiO_2(110).[36] As it is not possible in general to control the nature of the tip apex, it is of great benefit not only to

understand the zigzag contrast but also the various additional contrasts. At present, however, we do not have enough information to do this. Some combination of simultaneous NC-AFM/STM measurements, adsorption of probe molecules, and theoretical simulation of NC-AFM would likely shed light on the origin of the different contrasts.

Figure 5 shows three sequential NC-AFM images of the TiO_2(011)-(2×1) surface. The contrast is similar to that in Figure 4e,f in that the rows show no sub-row structure. However, while the hydrogen atoms appear as dark dumbbells in Figure 4e,f, in Figure 5, these adatoms appear as dark spots, offset to one side of the (2×1) row. In Figure 5b,c, most of the H adatoms remain in the same positions as those in Figure 5a except for the three that are circled.

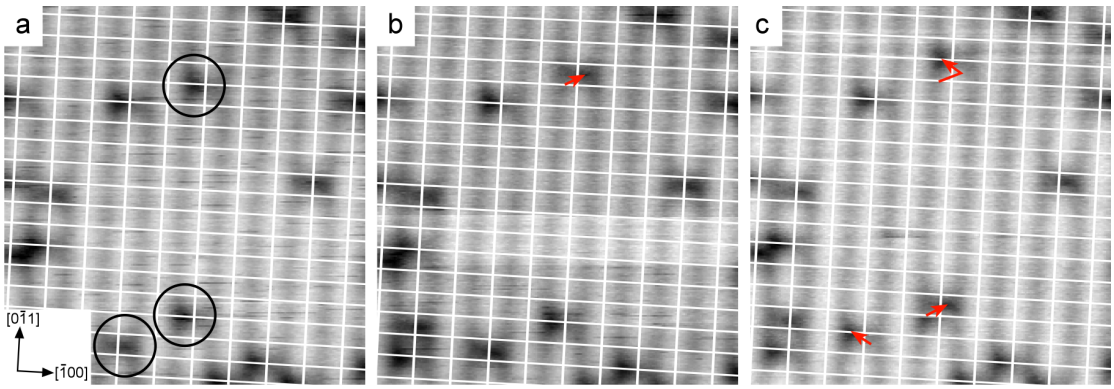

Figure 5 Sequential (88 Å × 92 Å) NC-AFM images (V_{CPD} = 1 V, Δf = -6.2 Hz) of the TiO_2(011)-(2×1) surface showing the diffusion of H adatoms. A grid is drawn over each image to show the primitive unit cells. All H adatoms remain in the same positions, except for those indicated with circles in (a). The red arrows show the displacements of the H adatoms with respect to their previous positions.

In the successive images, the paths of these H adatoms are indicated with red arrows. In each step, the H adatoms move up or down by half a unit cell in the [0$\bar{1}$1] direction, while also switching the direction in which they are offset. This leads to a zigzag pathway which can be explained on the basis of calculations reported by Tao *et al*.[14] An energy barrier of 0.75 eV is found for hydrogen diffusion from one top O site to another, i.e. from O(1) to O(1*) and vice versa and is expected to be accessible at room temperature. Indeed, this energy barrier is similar to that found experimentally for H diffusion on TiO_2(110).[38] Diffusion of hydrogen from the topmost O to the second layer of oxygen, i.e. O(2) and O(2*) has a higher barrier of 1.14 eV. As such, the easiest path for hydrogen diffusion is the zigzag along the topmost O atoms. We note also that the path for H diffusion highlighted in Figure 4c,d is also diagonal: the H adatom moves up or down the [0$\bar{1}$1] direction by half a unit cell while switching the side in which it is offset. Thus our observation of this zigzag pathway gives strong evidence for the adsorption of H adatoms on the topmost O atoms, O(1) and O(1*).

CONCLUSIONS

In conclusion, we have used NC-AFM and STM to study the rutile TiO_2(011)-(2×1) surface. NC-AFM images were obtained with several different contrasts. In particular, a zigzag contrast was observed that is similar to that commonly observed in STM images. Simultaneously-recorded NC-AFM and STM images indicate that the zigzags in NC-AFM and STM are in phase and may therefore have a similar origin. Hydrogen adatoms were also identified in NC-AFM images by comparison with STM. Sequential NC-AFM scans of the same area showed that the hydrogen atoms

readily diffuse between adjacent topmost oxygen atoms in a zigzag pathway that gives evidence for the adsorption of H adatoms on either side of the (2×1) rows.

Acknowledgements

The authors wish to thank Gilberto Teobaldi for supplying the simulated image in Figure 1c. This work was supported by Grants-in-Aid for JSPS Fellows (26-689) and for Scientific Research (25106002, 26110516, 26600015, 15H03566) from the Ministry of Education, Culture, Sports, Science, and Technology of Japan (MEXT). We also acknowledge financial support from the Asahi Glass Foundation, the Mitsubishi Foundation, and the Yamada Science Foundation.

Supporting Information Available: Figure S1 shows a number of NC-AFM images with contrast differing from those in the article. This information is available free of charge via the Internet at http://pubs.acs.org

References

(1) Fujishima, A.; Honda, K. Electrochemical Photolysis of Water at a Semiconductor Electrode. *Nature (London)* **1972**, *238*, 37-38.

(2) Diebold, U. The Surface Science of Titanium Dioxide. *Surf. Sci. Reports* **2003**, *48*, 53-229.

(3) Pang, C. L.; Lindsay, R.; Thornton, G. Structure of Clean and Adsorbate-Covered Single-Crystal Rutile TiO_2 Surfaces. *Chem. Rev.* **2013**, *113*, 3887-2948.

(4) Pang, C. L.; Thornton, G. The Many Faces of Rutile Titania. *Surf. Sci.* **2006**, *600*, 4405-4406.

(5) Beck, T.J.; Klust, A.; Batzill, M.; Diebold, U.; Di Valentin, C.; Selloni, A. Surface Structure of TiO_2(011)-(2 × 1). *Phys. Rev. Lett.* **2004**, *93*, 036104.

(6) Kubo, T.; Orita, H.; Nozoye, H. Surface Structures of Rutile TiO_2(011). *J. Am. Chem. Soc.* **2007**, *129*, 10474-10478.

(7) Dulub, O.; Di Valentin, C.; Selloni, A.; Diebold, U. Structure, Defects, and Impurities at the Rutile TiO_2(011)-(2 × 1) surface: A Scanning Tunneling Microscopy Study. *Surf. Sci.* **2006**, *600*, 4407-4417.

(8) Dulub, O.; Batzill, M.; Solovev, S.; Loginova, E.; Alchagirov, A.; Madey, T. E.; Diebold, U. Electron-Induced Oxygen Desorption from the TiO_2(011)-2×1 Surface Leads to Self-Organized Vacancies. *Science* **2009**, *317*, 1052-1056.

(9) Torrelles, X.; Cabailh, G.; Lindsay, R.; Bikondoa, O.; Roy, J.; Zegenhagen, J.; Teobaldi, G.; Hofer, W. A.; Thornton, G. Geometric Structure of TiO_2(011)(2 × 1). *Phys. Rev. Lett.* **2008**, *101*, 185501.

(10) Gong, X. -Q.; Khorshidi, N.; Stierle, A.; Vonk, V.; Ellinger, C.; Dosch, H.; Cheng, H.; Selloni, A.; He, Y.; Dulub, O.; Diebold, U. The 2 × 1 Reconstruction of the Rutile TiO_2(011) Surface: A Combined Density Functional Theory, X-ray Diffraction, and Scanning Tunneling Microscopy Study. *Surf. Sci.* **2009**, *603*, 138-144.

(11) Chamberlin, S. E.; Hirschmugl, C. J.; Poon, H. C.; Saldin, D. K. Geometric Structure of TiO_2(011)(2×1) Surface by Low Energy Electron Diffraction (LEED). *Surf. Sci.* **2009**, *603*, 3367-3373.

(12) Tekiel, A.; Godlewski, S.; Budzioch, J.; Szymonski, M. Nanofabrication of PTCDA Molecular Chains on Rutile TiO_2(011)-(2 × 1) Surfaces. *Nanotechnology*, **2008**, *19*, 496304.

(13) Tao, J.; Luttrell, T.; Batzill, M. A Two-Dimensional Phase of TiO_2 with a Reduced Bandgap. *Nat. Chem*. **2011**, *3*, 296-300.

(14) Tao, J.; Cuan, Q.; Gong, X. –Q.; Batzill, M. Diffusion and Reaction of Hydrogen on Rutile TiO_2(011)-2×1: The Role of Surface Structure. *J. Phys. Chem. C*. **2012**, *116*, 20438-20446.

(15) Woolcot, T.; Teobaldi, G.; Pang. C. L.; Beglitis, N. S.; Fisher, A. J.; Hofer, W. A.; Thornton G. Scanning Tunneling Microscopy Contrast Mechanisms for TiO_2. *Phys. Rev. Lett.* **2012**, *109*, 156105.

(16) Addou, R.; Senftle, T. P.; O'Connor, N.; Janik, M. J.; van Duin, A. C. T.; Batzill, M. Influence of Hydroxyls on Pd Atom Mobility and Clustering on Rutile TiO_2(011) - 2 × 1. ACS Nano **2014**, *8*, 6321-6333.

(17) Ariga, H.; Taniike, T.; Morikawa, H.; Tero, R.; Kondoh, H.; Iwasawa, Y. Lattice-Work Structure of a TiO_2(001) Surface Studied by STM, Core-Level Spectroscopies and DFT Calculations *Chem. Phys. Lett.* **2008**, *454*, 350-354.

(18) Uetsuka, H.; Henderson, M.A.; Sasahara, A.; Onishi, H. Formate Adsorption on the (111) Surface of Rutile TiO_2. *J. Phys. Chem. B* **2004**, *108*, 13706-13710.

(19) Setvín, M.; Aschauer, U.; Scheiber, P.; Li, Y. -F.; Hou, W.; Schmid, M.; Selloni, A.; Diebold, U. Reaction of O_2 with Subsurface Oxygen Vacancies on TiO_2 Anatase (101). *Science* **2013**, *341*, 988-991.

(20) De Angelis, F.; Di Valentin, C.; Fantacci, S.; Vittadini, A.; Selloni, A. Theoretical Studies on Anatase and Less Common TiO_2 Phases: Bulk, Surfaces, and Nanomaterials. *Chem. Rev.* **2014**, 114, 9708−9753.

(21) Wang, Y.; Sun, H.; Tan, S.; Feng, H.; Cheng, Z.; Zhao, J.; Zhao, A.; Wang, B.; Luo, Y.; Yang, J.; Hou, J. G. Role of Point Defects on the Reactivity of Reconstructed Anatase Titanium Dioxide (001) Surface. *Nat. Comm.* **2013**, *4*, 2214.

(22) Stetsovych, O.; Todorovic, M.; Shimizu, T. K.; Moreno, C.; Ryan, J. W.; León, C. P.; Sagisaka, K.; Palomares, E.; Matolín, V.; Fujita, D.; Perez, R.; Custance, O.

Atomic Species Identification at the (101) Anatase Surface by Simultaneous Scanning Tunneling and Atomic Force Microscopy, *Nat. Comm.* **2015**, *6*, 7265.

(23) Harrison, G. T.; Spadaro, M. C.; Pang, C. L.; Grinter, D. C.; Yim, C. M.; Luches, P.; Thornton, G. Lepidocrocite-like TiO_2 and TiO_2(110)–(1 × 2) supported on W(100). *Mater. Sci. Technol.* **2015** doi: 10.1179/1743284715Y.0000000086

(24) Rohrer, G. S. in The Chemical Physics of Solid Surfaces: Oxide Surfaces, edited by Woodruff, D. P. (Elsevier, Amsterdam, 2001), Vol. 9, Chap. 12.

(25) Ohno, T.; Sarukawa, K.; Matsumura, M. Crystal Faces of Rutile and Anatase TiO_2 Particles and their Roles in Photocatalytic Reactions. *New J. Chem.* **2002**, *26,* 1167-1170.

(26) Fernández-Torre, D.; Yurtsever, A.; Onoda, J.; Abe, M.; Morita, S.; Sugimoto, Y.; Pérez, R. Pt Atoms Adsorbed on TiO_2(110)-(1 × 1) Studied with Noncontact Atomic Force Microscopy and First-Principles Simulations. *Phys. Rev. B* **2015**, *91*, 075401.

(27) Enevoldsen, G. H.; Pinto, H. P.; Foster, A. S.; Jensen, M. C. R.; Hofer, W. A.; Hammer, B.; Lauritsen, J. V.; Besenbacher, F. Imaging of the Hydrogen Subsurface Site in Rutile TiO_2. *Phys. Rev. Lett.* **2010**, *104*, 119604.

(28) Sasahara, A.; Uetsuka, H.; Onishi, H. Individual Na Adatoms on TiO_2(110)-(1 × 1) Surface Observed using Kelvin Probe Force Microscope*Jpn. J. Appl. Phys.* **2004**, *43*, 4647.

(29) Yurtsever, A.; Sugimoto, Y.; Abe, M.; Morita, S. Alkali-Metal Adsorption and Manipulation on a Hydroxylated TiO_2(110) Surface using Atomic Force Microscopy. *Phys. Rev. B* **2011**, *84*, 085413.

(30) Chung, H. J.; Yurtsever, A.; Sugimoto, Y.; Abe, M.; Morita, S. Kelvin Probe Force Microscopy Characterization of TiO_2(110)-supported Au Clusters. *Appl. Phys. Lett.* **2011**, *99*, 123102.

(31) Pang, C. L.; Yurtsever, A.; Onoda, J.; Sugimoto, Y.; Thornton, G. ($2n \times 1$) Reconstructions of TiO_2(011) Revealed by Noncontact Atomic Force Microscopy and Scanning Tunneling Microscopy, *J. Phys. Chem. C* **2014**, *118*, 23168-23174

(32) Albrecht, T. R.; Grütter, P.; Horne, D.; Rugar, D. Frequency Modulation Detection using High-*Q* Cantilevers for Enhanced Force Microscope Sensitivity. *J. Appl. Phys*. **1991**, *69*, 668-673.

(33) Pang, C. L.; Sasahara, A.; Onishi, H.; Chen, Q.; Thornton, G. Noncontact Atomic Force Microscopy Imaging of Water Dissociation Products on TiO_2(110). *Phys. Rev. B* **2006**, *74*, 073411.

(34) Yurtsever, A.; Fernández-Torre, D.; González, C.; Jelínek, P.; Pou, P.; Sugimoto, Y. Abe, M.; Pérez, R.; Morita, S. Understanding Image Contrast Formation in TiO_2 with Force Spectroscopy. *Phys. Rev. B* **2012**, *85*, 125416.

(35) Lauritsen, J. V; Foster, A. S; Olesen, G. H.; Christensen, M. C.; Kühnle, A.; Helveg, S.; Rostrup-Nielson, J. R.; Clausen, B. S.; Reichling, M.; Besenbacher, F. Chemical Identification of Point Defects and Adsorbates on a Metal Oxide Surface by Atomic Force Microscopy. *Nanotechnology*, **2006**, *17*, 3436-3441.

(36) Yurtsever, A.; Sugimoto, Y.; Abe, M.; Morita, S. NC-AFM Imaging of the TiO_2(110)-(1×1) Surface at Low Temperature. *Nanotechnology*, **2010**, *21*, 165702.

(37) Onoda, J.; Pang, C. L.; Yurtsever, A.; Sugimoto, Y. Subsurface Charge Repulsion of Adsorbed H-Adatoms on TiO_2 (110). *J. Phys. Chem. C.* **2014**, 118, 13674-79.

(38) Li, S. C.; Zhang, Z.; Sheppard, D.; Kay, B. D.; White, J. M.; Du, Y.; Lyubinetsky, I.; Henkelman, G.; Dohnálek, Z. Intrinsic Diffusion of Hydrogen on Rutile TiO_2(110). *J. Am. Chem. Soc.* **2008**, *130*, 9080-9088.